The thermo-Alfvénic instability — from toy model to torus

T. Adkins[1,2], P. G. Ivanov[2], D. Kennedy[3], M. Giacomin[4],
A. A. Schekochihin[2], and many others

[1]Department of Physics, University of Otago,
Dunedin, 9016, NZ

[2]Rudolf Peierls Centre For Theoretical Physics,
University of Oxford,
Oxford, OX1 3PU, UK

[3]UK Atomic Energy Authority,
United Kingdom Atomic Energy Authority,
Abingdon, OX14 3EB, UK

[4]Dipartimento di Fisica "G. Galilei"
Università degli Studi di Padova
Padova, Italy

PPPL Theory seminar, 16/04/2024

Table of Contents

Table of Contents

Plasma losses

- **Turbulent transport** is expected to be the dominant mechanism of heat and particle losses in tokamaks, as well as neoclassically optimised stellarators.

Plasma losses

- **Turbulent transport** is expected to be the dominant mechanism of heat and particle losses in tokamaks, as well as neoclassically optimised stellarators.

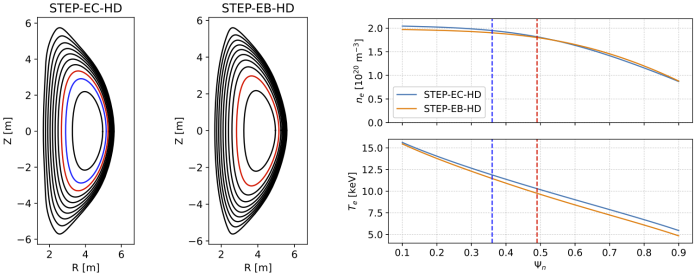

Figure 1: STEP equilibria from Kennedy et al. (2023)

Plasma losses

- **Turbulent transport** is expected to be the dominant mechanism of heat and particle losses in tokamaks, as well as neoclassically optimised stellarators.

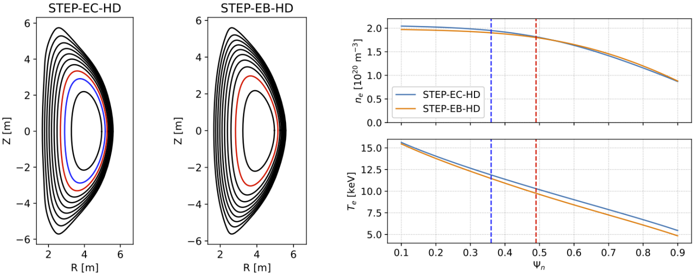

Figure 1: STEP equilibria from Kennedy et al. (2023)

- Radial gradient of the plasma pressure is a **source of free-energy** for unstable perturbations, typically on scales comparable to the particle gyroradii

$$k_\parallel L \sim 1, \quad k_\perp \rho_s \sim 1 \quad \Rightarrow \quad \frac{k_\parallel}{k_\perp} \sim \frac{\rho_s}{L} \ll 1 \quad \Rightarrow \quad \text{gyrokinetics}$$

Plasma losses

- **Turbulent transport** is expected to be the dominant mechanism of heat and particle losses in tokamaks, as well as neoclassically optimised stellarators.

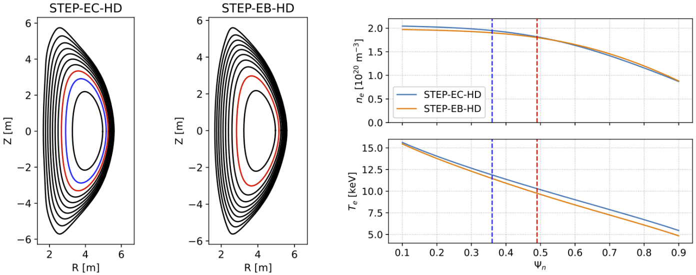

Figure 1: STEP equilibria from Kennedy et al. (2023)

- Radial gradient of the plasma pressure is a **source of free-energy** for unstable perturbations, typically on scales comparable to the particle gyroradii
- Understanding the microinstability properties of tokamak plasmas, and the resultant turbulence, is key to successful reactor design.

Electromagnetic fluctuations

- Electromagnetic fluctuations will be larger in reactor-relevant tokamak scenarios due to a higher values of the **plasma beta**:

$$\beta_s = \frac{\text{thermal pressure}}{\text{magnetic pressure}} = \frac{8\pi n_{0s} T_{0s}}{B_0^2}.$$

Electromagnetic fluctuations

- Electromagnetic fluctuations will be larger in reactor-relevant tokamak scenarios due to a higher values of the **plasma beta**:

$$\beta_s = \frac{\text{thermal pressure}}{\text{magnetic pressure}} = \frac{8\pi n_{0s} T_{0s}}{B_0^2}.$$

- This is particularly true for spherical-tokamak (ST) designs, e.g., MAST, STEP, NSTX-U, and ST40.

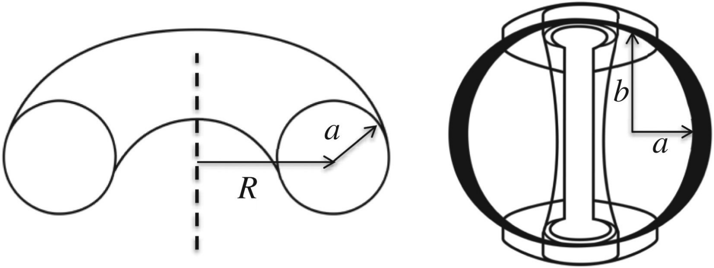

Figure 2: From Costley (2019)

ST confinement scaling

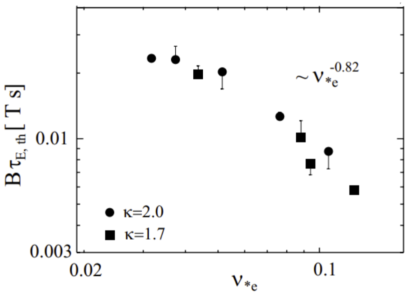

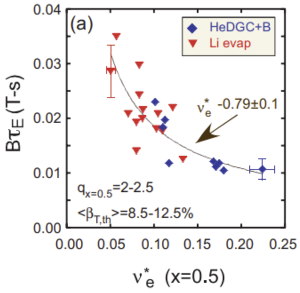

Figure 3: From Valovič et al. (2011) (left), Kaye et al. (2013) (right)

ST confinement scaling

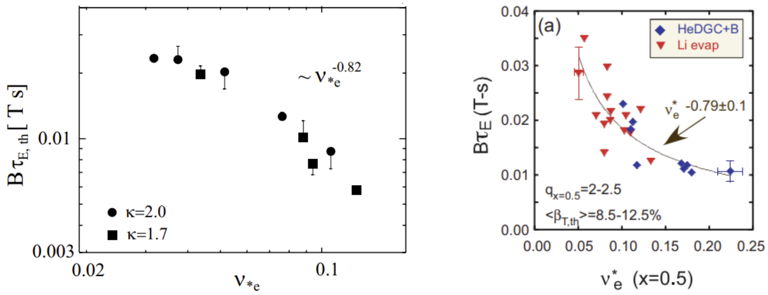

Figure 3: From Valovič et al. (2011) (left), Kaye et al. (2013) (right)

- Experimental MAST and NSTX data demonstrated a favourable scaling of confinement time with normalised collisionality:

$$B\tau_E \sim \nu_*^{-0.8\pm0.1}$$

ST confinement scaling

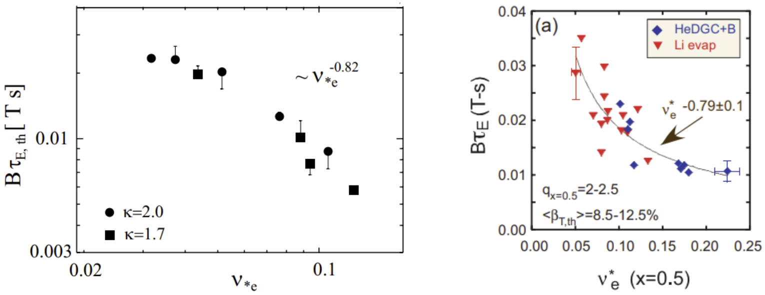

Figure 3: From Valovič et al. (2011) (left), Kaye et al. (2013) (right)

- Experimental MAST and NSTX data demonstrated a favourable scaling of confinement time with normalised collisionality:

$$B\tau_E \sim \nu_*^{-0.8\pm0.1}$$

- Shown to be *consistent* with the stabilisation of core micro-tearing modes, and a subsequent reduction in electron turbulent transport, at lower ν_*.

Unfinished business...

- Problem solved?

Unfinished business...

- Problem solved? No!

Unfinished business...

- Problem solved? No!
- **Uncertainty** about the fundamental physics responsible for commonly observed electromagnetic modes, e.g., the

micro-tearing mode (MTM)	or	kinetic ballooning mode (KBM)

Unfinished business...

- Problem solved? No!
- **Uncertainty** about the fundamental physics responsible for commonly observed electromagnetic modes, e.g., the

micro-tearing mode (MTM)	or	kinetic ballooning mode (KBM)

- Nonlinear simulations of local gyrokinetic turbulence sometimes **fail to saturate** at an experimentally-permissible level in the electromagnetic regime; see, e.g., Pueschel et al. (2013); Giacomin et al. (2023).

Unfinished business...

- Problem solved? No!
- **Uncertainty** about the fundamental physics responsible for commonly observed electromagnetic modes, e.g., the

micro-tearing mode (MTM)	or	kinetic ballooning mode (KBM)

- Nonlinear simulations of local gyrokinetic turbulence sometimes **fail to saturate** at an experimentally-permissible level in the electromagnetic regime; see, e.g., Pueschel et al. (2013); Giacomin et al. (2023).
- Not just a problem for STs; we are projected to have $\beta_e \approx 2.5\%$ in ITER, where electromagnetic effects will be important.

Unfinished business...

- Problem solved? No!
- **Uncertainty** about the fundamental physics responsible for commonly observed electromagnetic modes, e.g., the

micro-tearing mode (MTM)	or	kinetic ballooning mode (KBM)

- Nonlinear simulations of local gyrokinetic turbulence sometimes **fail to saturate** at an experimentally-permissible level in the electromagnetic regime; see, e.g., Pueschel et al. (2013); Giacomin et al. (2023).
- Not just a problem for STs; we are projected to have $\beta_e \approx 2.5\%$ in ITER, where electromagnetic effects will be important.
- Key question:

> Can we distil the **essential physical ingredients** behind electromagnetic destabilisation by constructing simplified models?

Table of Contents

Local constant-curvature approximation

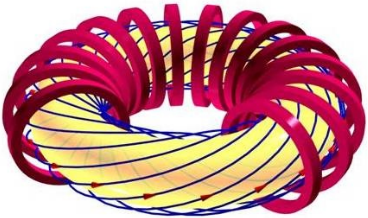

Local constant-curvature approximation

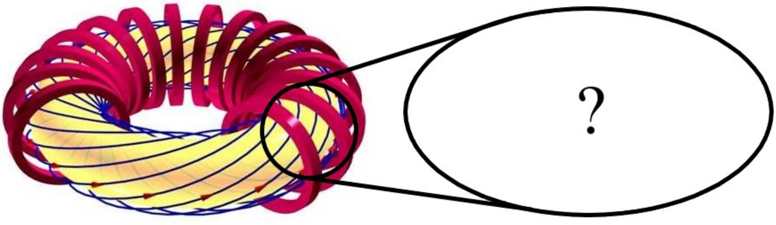

Local constant-curvature approximation

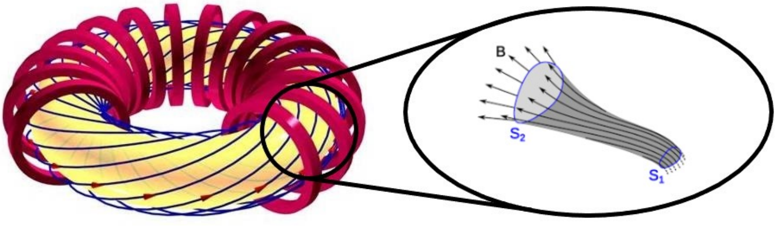

Local constant-curvature approximation

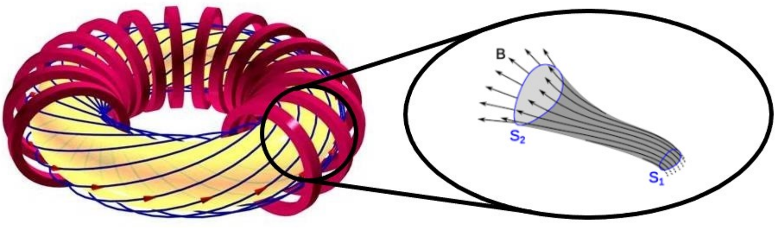

- These systems are incredibly complicated; what methods can we use to better understand them?

Local constant-curvature approximation

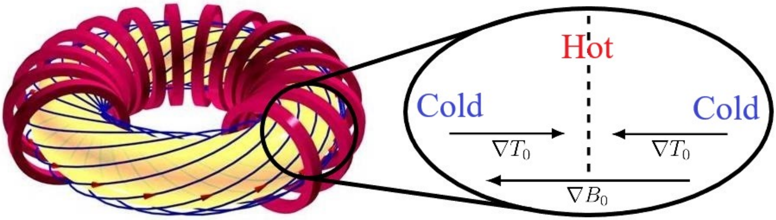

- These systems are incredibly complicated; what methods can we use to better understand them?
- Tokamak instabilities are distinguished from other plasma instabilities by the particular **configuration of equilibrium gradients**

Local constant-curvature approximation

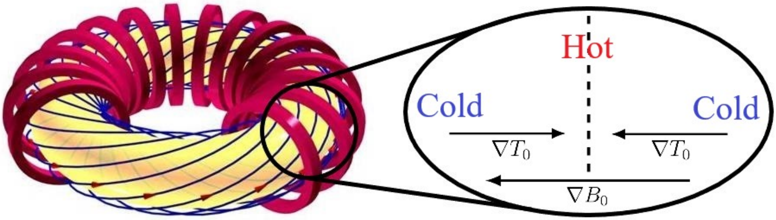

- These systems are incredibly complicated; what methods can we use to better understand them?
- Tokamak instabilities are distinguished from other plasma instabilities by the particular **configuration of equilibrium gradients**
- Consider a local "toy" model with radial equilibrium gradients that are constant along the field line:

$$L_T^{-1} = -\frac{1}{T_{0e}}\frac{\mathrm{d}T_{0e}}{\mathrm{d}x}, \quad L_B^{-1} = -\frac{1}{B_0}\frac{\mathrm{d}B_0}{\mathrm{d}x}.$$

Low-beta electron dynamics

- All that follows is derived in an asymptotic limit of gyrokinetics.

Equilibrium parameters:	
Fields:	
Frequencies:	
Lengthscales:	

Low-beta electron dynamics

- All that follows is derived in an asymptotic limit of gyrokinetics.

Equilibrium parameters:	$m_e/m_i \lesssim \beta_e \ll 1, \quad L_B/L_T \sim 1$
Fields:	
Frequencies:	
Lengthscales:	

Low-beta electron dynamics

- All that follows is derived in an asymptotic limit of gyrokinetics.

Equilibrium parameters:	$m_e/m_i \lesssim \beta_e \ll 1, \quad L_B/L_T \sim 1$
Fields:	$\phi,\ A_\parallel,\ \cancel{\delta B_\parallel},\ \delta n_e,\ u_{\parallel e},\ \delta T_e,\ \ldots$
Frequencies:	
Lengthscales:	

- Low-beta limit orders out parallel (compressive) magnetic-field perturbations. Not always a good approximation; e.g., in STEP (see Kennedy et al., 2024)

Low-beta electron dynamics

- All that follows is derived in an asymptotic limit of gyrokinetics.

Equilibrium parameters:	$m_e/m_i \lesssim \beta_e \ll 1, \quad L_B/L_T \sim 1$
Fields:	$\phi,\ A_\parallel,\ \cancel{\delta B_\parallel},\ \delta n_e,\ u_{\parallel e},\ \delta T_e,\ \dots$
Frequencies:	$\omega \sim k_\parallel v_{\mathrm{the}} \sim \omega_{*e} \sim \omega_{de} \sim k_\parallel v_A$
Lengthscales:	

- Low-beta limit orders out parallel (compressive) magnetic-field perturbations. Not always a good approximation; e.g., in STEP (see Kennedy et al., 2024)
- Considering timescales comparable to the electron streaming rate; appropriate for electron-scale instabilities.

Low-beta electron dynamics

- All that follows is derived in an asymptotic limit of gyrokinetics.

Equilibrium parameters:	$m_e/m_i \lesssim \beta_e \ll 1, \quad L_B/L_T \sim 1$
Fields:	$\phi,\ A_\parallel,\ \cancel{\delta B_\parallel},\ \delta n_e,\ u_{\parallel e},\ \delta T_e,\ \ldots$
Frequencies:	$\omega \sim k_\parallel v_{\mathrm{the}} \sim \omega_{*e} \sim \omega_{de} \sim k_\parallel v_A$
Lengthscales:	$\rho_i^{-1} \lesssim k_\perp \sim d_e^{-1} \ll \rho_e^{-1}, \quad k_\parallel L_T \sim \sqrt{\beta_e}$

- Low-beta limit orders out parallel (compressive) magnetic-field perturbations. Not always a good approximation; e.g., in STEP (see Kennedy et al., 2024)
- Considering timescales comparable to the electron streaming rate; appropriate for electron-scale instabilities.
- In a straight (unsheared) magnetic field, the **flux-freezing scale** $d_e = \rho_e/\sqrt{\beta_e}$ demarcates the transition between the electrostatic and electromagnetic regimes.

Electrostatic regime

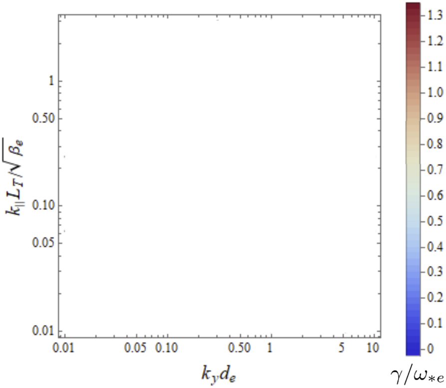

Electrostatic regime

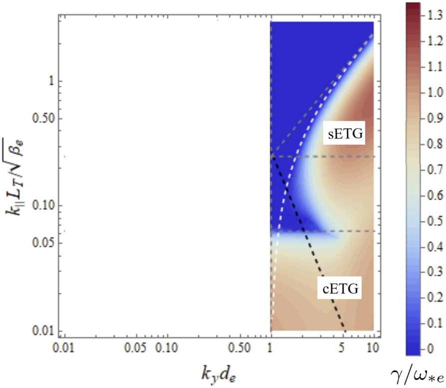

- At $k_\perp d_e \gg 1$, electrons are allowed to stream freely across unperturbed field lines. Instabilities extract free energy from the ETG via the usual $\boldsymbol{E} \times \boldsymbol{B}$ **feedback** mechanism.

Electrostatic regime

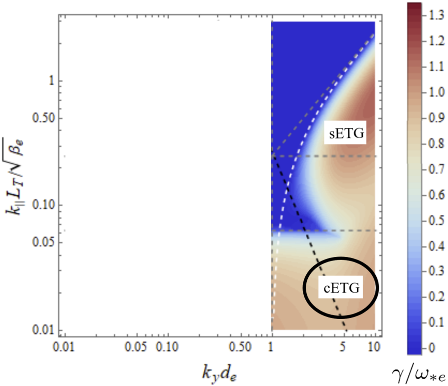

- At $k_\perp d_e \gg 1$, electrons are allowed to stream freely across unperturbed field lines. Instabilities extract free energy from the ETG via the usual $\boldsymbol{E} \times \boldsymbol{B}$ **feedback** mechanism.
- For $k_\parallel \to 0$, we recover the familiar curvature-mediated ETG (2D interchange mode, Horton et al. 1988):

$$\omega = \pm i \left(2\omega_{de}\omega_{*e}\bar{\tau}\right)^{1/2}.$$

Curvature-mediated ETG

$$\underbrace{\frac{\mathrm{d}}{\mathrm{d}t}\frac{\delta n_e}{n_{0e}} = -\frac{\rho_e v_{\mathrm{the}}}{L_B}\frac{\partial}{\partial y}\frac{\delta T_e}{T_{0e}}}_{\text{Continuity}}, \quad \underbrace{\frac{\mathrm{d}}{\mathrm{d}t}\frac{\delta T_e}{T_{0e}} = -\frac{\rho_e v_{\mathrm{the}}}{2L_T}\frac{\partial \varphi}{\partial y}}_{\text{Temp. advection by } \boldsymbol{E}\times\boldsymbol{B}},$$

Curvature-mediated ETG

$$\underbrace{\frac{\mathrm{d}}{\mathrm{d}t}\frac{\delta n_e}{n_{0e}} = -\frac{\rho_e v_{\mathrm{the}}}{L_B}\frac{\partial}{\partial y}\frac{\delta T_e}{T_{0e}}}_{①}, \quad \frac{\mathrm{d}}{\mathrm{d}t}\frac{\delta T_e}{T_{0e}} = -\frac{\rho_e v_{\mathrm{the}}}{2L_T}\frac{\partial \varphi}{\partial y},$$

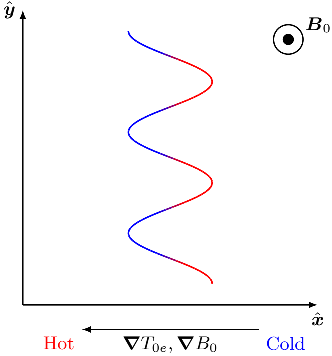

- A temperature perturbation with $k_y \neq 0$ has alternating hot and cold regions along $\hat{\boldsymbol{y}}$.

Curvature-mediated ETG

$$\underbrace{\frac{\mathrm{d}}{\mathrm{d}t}\frac{\delta n_e}{n_{0e}} = -\frac{\rho_e v_{\mathrm{the}}}{L_B}\frac{\partial}{\partial y}\frac{\delta T_e}{T_{0e}}}_{①}, \quad \frac{\mathrm{d}}{\mathrm{d}t}\frac{\delta T_e}{T_{0e}} = -\frac{\rho_e v_{\mathrm{the}}}{2L_T}\frac{\partial \varphi}{\partial y},$$

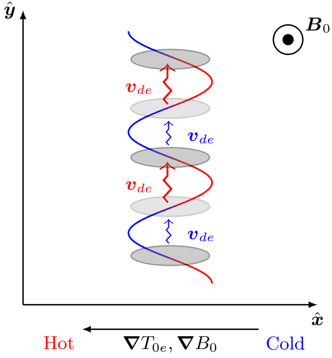

- Velocity dependence of magnetic drifts $\boldsymbol{v}_{de}$ creates an electron density perturbation (hot particles drift faster than cold ones).
- This electron density perturbation has only $k_y \neq 0$.

Curvature-mediated ETG

$$\frac{\mathrm{d}}{\mathrm{d}t}\frac{\delta n_e}{n_{0e}} = -\frac{\rho_e v_{\mathrm{the}}}{L_B}\frac{\partial}{\partial y}\frac{\delta T_e}{T_{0e}}, \quad \underbrace{\frac{\mathrm{d}}{\mathrm{d}t}\frac{\delta T_e}{T_{0e}} = -\frac{\rho_e v_{\mathrm{the}}}{2L_T}\frac{\partial \varphi}{\partial y}}_{②},$$

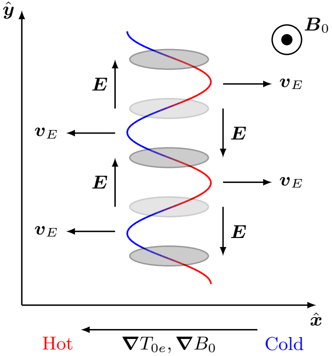

- The electron density perturbation creates, via a quasineutral Boltzmann-ion response, alternating electric fields $\boldsymbol{E}$.
- Gives rise to an $\boldsymbol{E} \times \boldsymbol{B}$ drift that reinforces the initial perturbation.

Electromagnetic regime

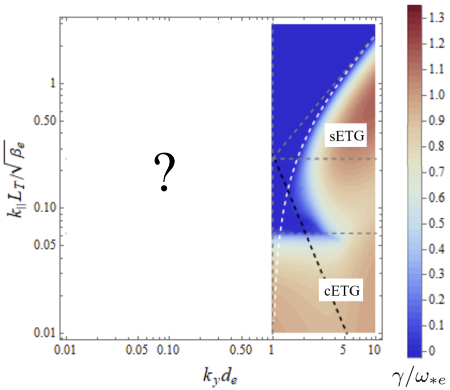

Electromagnetic regime

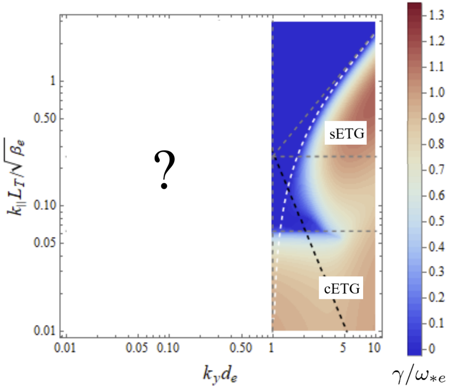

- At $k_\perp d_e \ll 1$, $\delta \boldsymbol{B}_\perp$ is created as electrons drag field lines around.

Electromagnetic regime

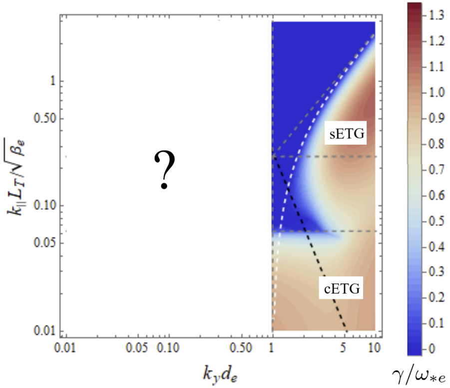

- At $k_\perp d_e \ll 1$, $\delta \boldsymbol{B}_\perp$ is created as electrons drag field lines around.
- Modifies parallel gradients, e.g.,

$$\frac{1}{T_{0e}} \boldsymbol{\nabla}_\parallel (T_{0e} + \delta T_e) = \boldsymbol{\nabla}_\parallel \frac{\delta T_e}{T_{0e}} + \frac{\delta B_x}{B_0} \frac{1}{T_{0e}} \frac{\mathrm{d}T_{0e}}{\mathrm{d}x} = \boldsymbol{\nabla}_\parallel \frac{\delta T_e}{T_{0e}} - \frac{\rho_e}{L_T} \frac{\partial \mathcal{A}}{\partial y}$$

$\Rightarrow$ introduces another mechanism by which the perturbations can go unstable.

Electromagnetic regime

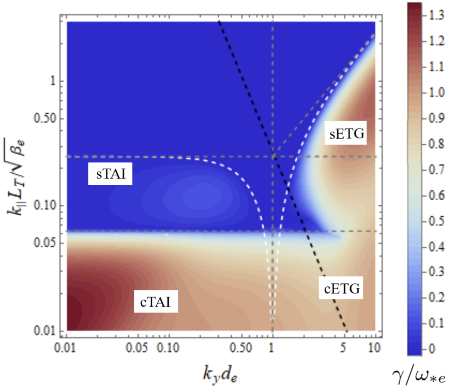

- At $k_\perp d_e \ll 1$, $\delta \boldsymbol{B}_\perp$ is created as electrons drag field lines around.
- Modifies parallel gradients, e.g.,

$$\frac{1}{T_{0e}}\nabla_\parallel(T_{0e}+\delta T_e) = \nabla_\parallel \frac{\delta T_e}{T_{0e}} + \frac{\delta B_x}{B_0}\frac{1}{T_{0e}}\frac{\mathrm{d}T_{0e}}{\mathrm{d}x} = \nabla_\parallel \frac{\delta T_e}{T_{0e}} - \frac{\rho_e}{L_T}\frac{\partial \mathcal{A}}{\partial y}$$

$\Rightarrow$ introduces another mechanism by which the perturbations can go unstable.

Electromagnetic regime

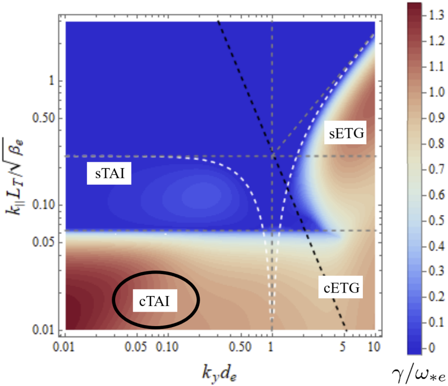

- Curvature-mediated ***thermo-Alfvénic instability*** (cTAI):

$$\omega = \pm i \left[2\omega_{de}\omega_{*e}(1+\bar{\tau})\right]^{1/2}.$$

- Two key differences to cETG: (i) it relies on $k_\parallel \neq 0$, and (ii) it does not require the $\boldsymbol{E} \times \boldsymbol{B}$ feedback mechanism to be unstable.

Curvature-mediated TAI

$$\underbrace{\frac{\mathrm{d}}{\mathrm{d}t}\frac{\delta n_e}{n_{0e}} = -\frac{\rho_e v_{\mathrm{the}}}{L_B}\frac{\partial}{\partial y}\frac{\delta T_e}{T_{0e}}}_{\text{Continuity}}, \quad \underbrace{\frac{\mathrm{d}\mathcal{A}}{\mathrm{d}t} + \frac{v_{\mathrm{the}}}{2}\frac{\partial \varphi}{\partial z} = \frac{v_{\mathrm{the}}}{2}\boldsymbol{\nabla}_{\parallel}\frac{\delta n_e}{n_{0e}}}_{\text{Parallel pressure balance}}, \quad \underbrace{\boldsymbol{\nabla}_{\parallel}\frac{\delta T_e}{T_{0e}} = \frac{\rho_e}{L_T}\frac{\partial \mathcal{A}}{\partial y}}_{\text{Isothermality}},$$

Curvature-mediated TAI

$$\frac{\mathrm{d}}{\mathrm{d}t}\frac{\delta n_e}{n_{0e}} = -\frac{\rho_e v_{\mathrm{th}e}}{L_B}\frac{\partial}{\partial y}\frac{\delta T_e}{T_{0e}}, \quad \frac{\mathrm{d}\mathcal{A}}{\mathrm{d}t} + \frac{v_{\mathrm{th}e}}{2}\frac{\partial \varphi}{\partial z} = \frac{v_{\mathrm{th}e}}{2}\boldsymbol{\nabla}_\parallel \frac{\delta n_e}{n_{0e}}, \quad \underbrace{\boldsymbol{\nabla}_\parallel \frac{\delta T_e}{T_{0e}} = \frac{\rho_e}{L_T}\frac{\partial \mathcal{A}}{\partial y}}_{①},$$

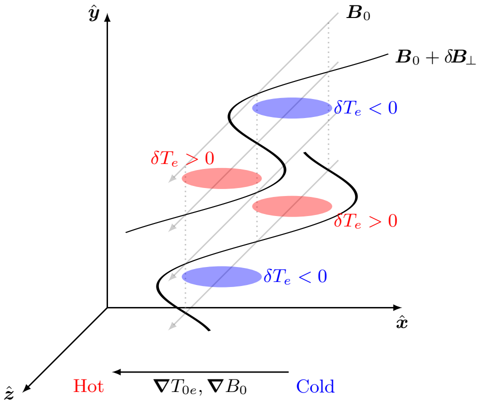

- A perturbation $\delta B_x = B_0 \rho_e \partial_y \mathcal{A}$ sets up a variation of total temp. along the perturbed field line as it makes excursions into hot and cold regions.
- Rapid thermal conduction along field lines creates a temperature perturbation that compensates for this.

Curvature-mediated TAI

$$\underbrace{\frac{\mathrm{d}}{\mathrm{d}t}\frac{\delta n_e}{n_{0e}} = -\frac{\rho_e v_{\mathrm{the}}}{L_B}\frac{\partial}{\partial y}\frac{\delta T_e}{T_{0e}},}_{②} \quad \frac{\mathrm{d}\mathcal{A}}{\mathrm{d}t} + \frac{v_{\mathrm{the}}}{2}\frac{\partial \varphi}{\partial z} = \frac{v_{\mathrm{the}}}{2}\boldsymbol{\nabla}_{\parallel}\frac{\delta n_e}{n_{0e}}, \quad \boldsymbol{\nabla}_{\parallel}\frac{\delta T_e}{T_{0e}} = \frac{\rho_e}{L_T}\frac{\partial \mathcal{A}}{\partial y},$$

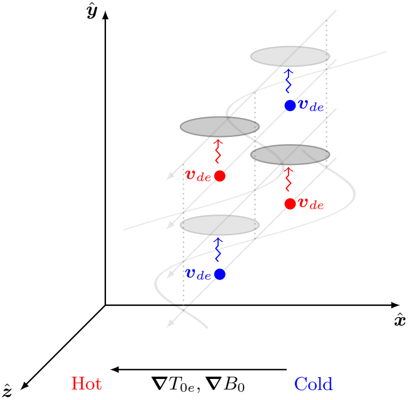

- Velocity dependence of magnetic drifts $\boldsymbol{v}_{de}$ creates an electron density perturbation (hot particles drift faster than cold ones).
- This electron density perturbation has both $k_y \neq 0$ and $k_{\parallel} \neq 0$.

Curvature-mediated TAI

$$\frac{\mathrm{d}}{\mathrm{d}t}\frac{\delta n_e}{n_{0e}} = -\frac{\rho_e v_{\mathrm{th}e}}{L_B}\frac{\partial}{\partial y}\frac{\delta T_e}{T_{0e}}, \quad \underbrace{\frac{\mathrm{d}\mathcal{A}}{\mathrm{d}t} + \frac{v_{\mathrm{th}e}}{2}\frac{\partial \varphi}{\partial z} = \frac{v_{\mathrm{th}e}}{2}\boldsymbol{\nabla}_\parallel \frac{\delta n_e}{n_{0e}}}_{③}, \quad \boldsymbol{\nabla}_\parallel \frac{\delta T_e}{T_{0e}} = \frac{\rho_e}{L_T}\frac{\partial \mathcal{A}}{\partial y},$$

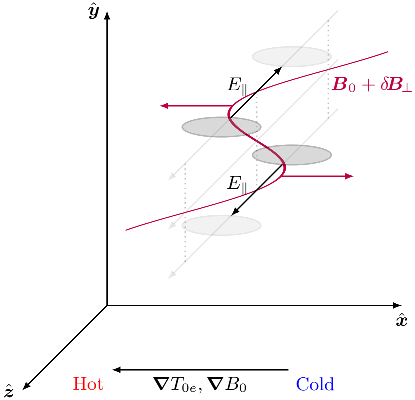

- The parallel density gradient must be balanced by the parallel electric field.
- Inductive part leads to an increase in δB_x, deforming the field line further into the hot and cold regions $\Rightarrow$ feedback.

Electron-scale instabilities: ETG and TAI

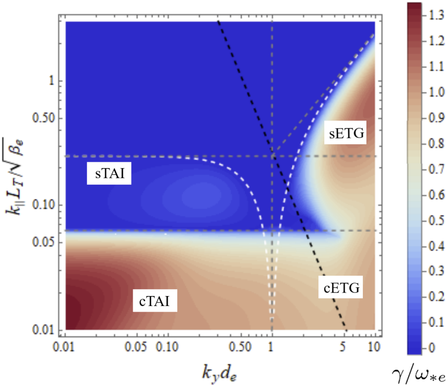

Electron-scale instabilities: ETG and TAI

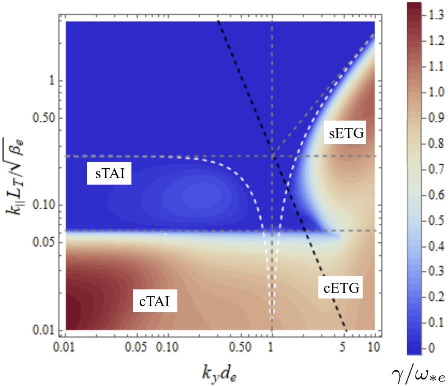

- Both the sTAI and cTAI exist in the collisionless ($\nu_* \to 0$) and collisional ($\nu_* \gg 1$) limits, with the relevant parallel timescale being parallel streaming and thermal conduction, respectively (see Adkins et al., 2022).

Electron-scale instabilities: ETG and TAI

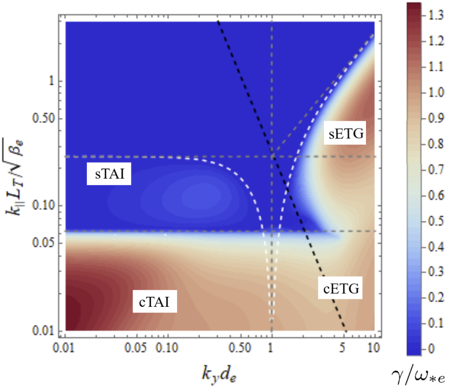

- Both the sTAI and cTAI exist in the collisionless ($\nu_* \to 0$) and collisional ($\nu_* \gg 1$) limits, with the relevant parallel timescale being parallel streaming and thermal conduction, respectively (see Adkins et al., 2022).
- The general physical mechanism behind the **thermo-Alfvénic instability** is the competition between the diamagnetic drifts and temperature equilibration along perturbed magnetic field lines $\Rightarrow$ magnetic flutter drive.

Table of Contents

Benchmarking against known results

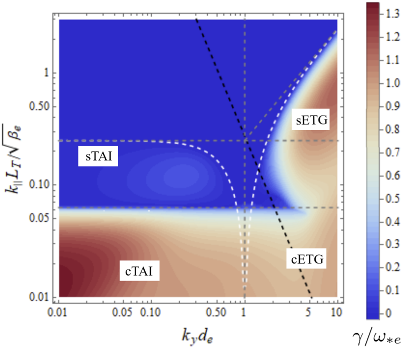

- Can we recover the TAI in gyrokinetics? Following results are from a collaboration with D. Kennedy (CCFE) and M. Giacomin (Padova)

Benchmarking against known results

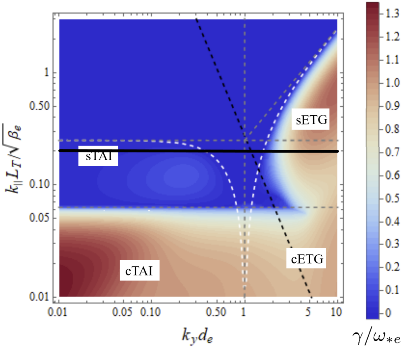

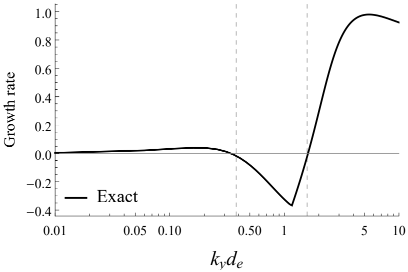

- Can we recover the TAI in gyrokinetics? Following results are from a collaboration with D. Kennedy (CCFE) and M. Giacomin (Padova)

Benchmarking against known results

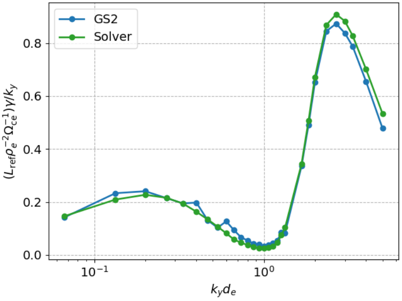

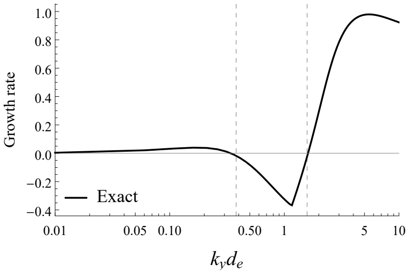

- Performed simulations of sTAI in `GS2` and `GENE`. Adiabatic ions, $\beta_e = 0.09$, $L_{\mathrm{ref}}/L_T = 105$, $k_\parallel^{\mathrm{min}} = 0.03\sqrt{\beta_e}/L_T$.

Benchmarking against known results

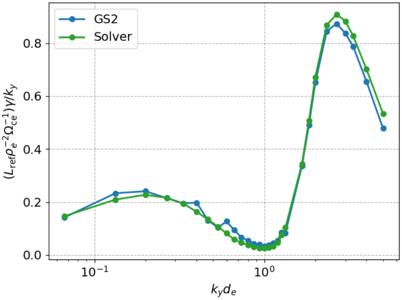

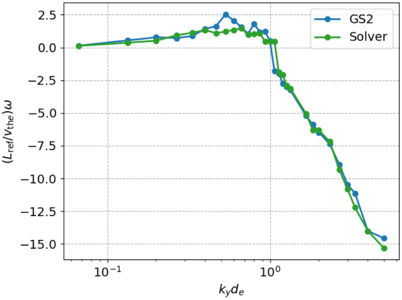

- Performed simulations of sTAI in `GS2` and `GENE`. Adiabatic ions, $\beta_e = 0.09$, $L_{\mathrm{ref}}/L_T = 105$, $k_\parallel^{\mathrm{min}} = 0.03\sqrt{\beta_e}/L_T$.

Benchmarking against known results

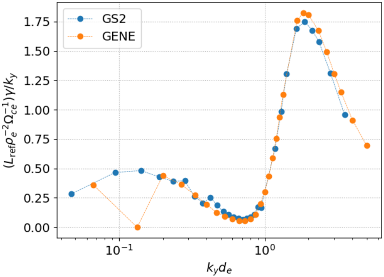

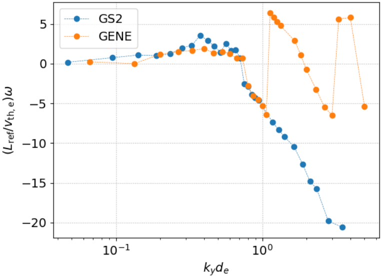

- Performed simulations of sTAI in `GS2` and `GENE`. Adiabatic ions, $\beta_e = 0.09$, $L_{\mathrm{ref}}/L_T = 105$, $k_\parallel^{\mathrm{min}} = 0.03\sqrt{\beta_e}/L_T$.

Benchmarking against known results

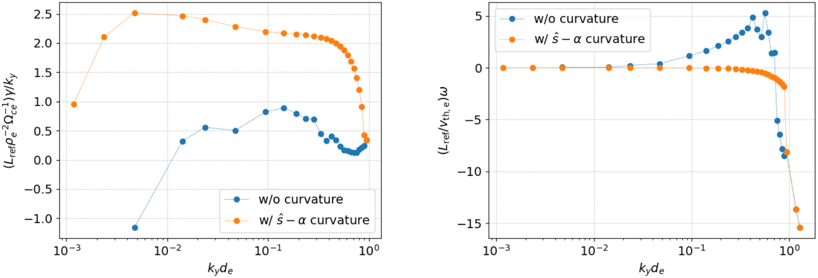

- Performed simulations of sTAI in `GS2` and `GENE`. Adiabatic ions, $\beta_e = 0.09$, $L_{\mathrm{ref}}/L_T = 105$, $k_\parallel^{\mathrm{min}} = 0.03\sqrt{\beta_e}/L_T$.
- What about **curvature**? Both `GS2` and `GENE` are able to recover cTAI in $\hat{s}-\alpha$ geometry with $q_0 = 1$, $r/R = 10^{-8}$.

Benchmarking against known results

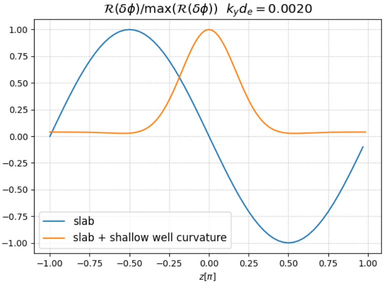

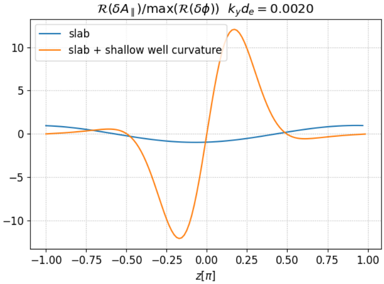

- Performed simulations of sTAI in **GS2** and **GENE**. Adiabatic ions, $\beta_e = 0.09$, $L_{\rm ref}/L_T = 105$, $k_\parallel^{\rm min} = 0.03\sqrt{\beta_e}/L_T$.
- What about **curvature**? Both **GS2** and **GENE** are able to recover cTAI in $\hat{s} - \alpha$ geometry with $q_0 = 1$, $r/R = 10^{-8}$.
- Eigenfunctions: sTAI has odd (tearing) parity, while cTAI has even parity.

Inching towards the torus

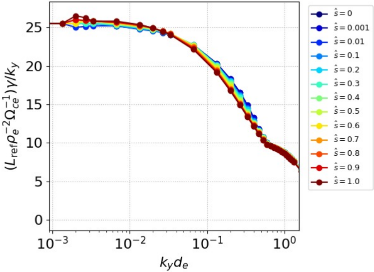

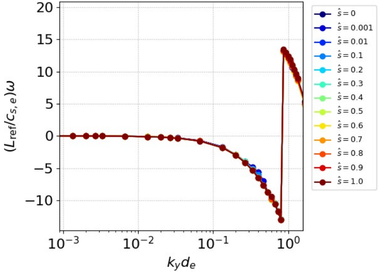

- Increase **complexity** further to better approximate a realistic tokamak: **magnetic shear** + **Shafranov shift.**

$$\hat{s} = \frac{r}{q}\frac{\mathrm{d}q}{\mathrm{d}r}, \qquad \alpha = -R_0 q^2 \frac{8\pi}{B_0^2}\frac{\mathrm{d}p}{\mathrm{d}r}$$

Inching towards the torus

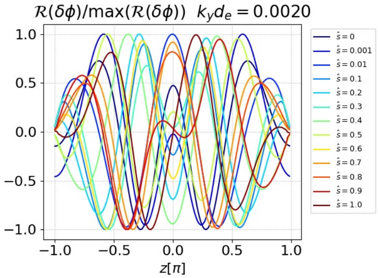

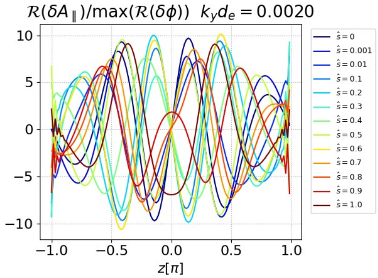

- Increase **complexity** further to better approximate a realistic tokamak: **magnetic shear** + **Shafranov shift.**

$$\hat{s} = \frac{r}{q}\frac{\mathrm{d}q}{\mathrm{d}r}, \qquad \alpha = -R_0 q^2 \frac{8\pi}{B_0^2}\frac{\mathrm{d}p}{\mathrm{d}r}$$

Inching towards the torus

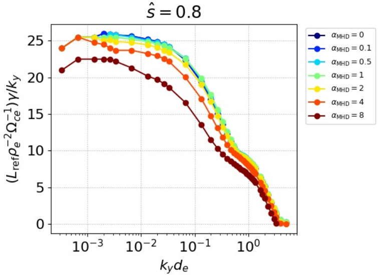

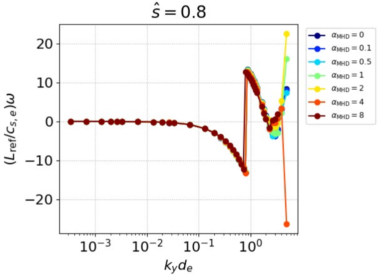

- Increase **complexity** further to better approximate a realistic tokamak: magnetic shear + **Shafranov shift.**

$$\hat{s} = \frac{r}{q}\frac{\mathrm{d}q}{\mathrm{d}r}, \qquad \alpha = -R_0 q^2 \frac{8\pi}{B_0^2}\frac{\mathrm{d}p}{\mathrm{d}r}$$

Inching towards the torus

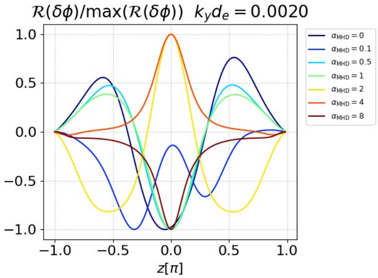

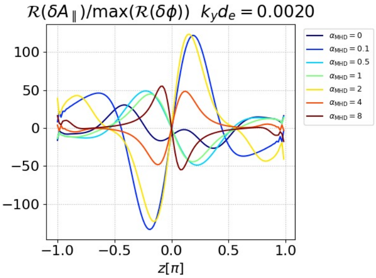

- Increase **complexity** further to better approximate a realistic tokamak: magnetic shear + **Shafranov shift.**

$$\hat{s} = \frac{r}{q}\frac{\mathrm{d}q}{\mathrm{d}r}, \qquad \alpha = -R_0 q^2 \frac{8\pi}{B_0^2}\frac{\mathrm{d}p}{\mathrm{d}r}$$

Inching towards the torus

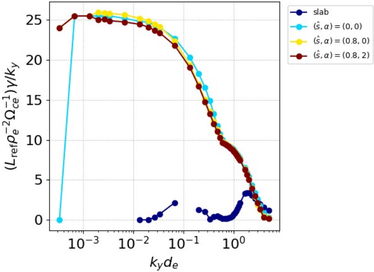

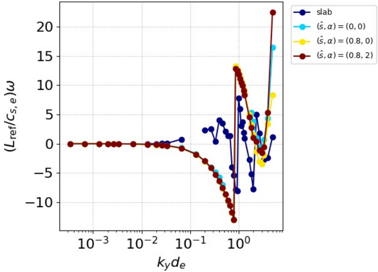

- Increase **complexity** further to better approximate a realistic tokamak: **magnetic shear + Shafranov shift.**

$$\hat{s} = \frac{r}{q} \frac{\mathrm{d}q}{\mathrm{d}r}, \quad \alpha = -R_0 q^2 \frac{8\pi}{B_0^2} \frac{\mathrm{d}p}{\mathrm{d}r}$$

Inching towards the torus

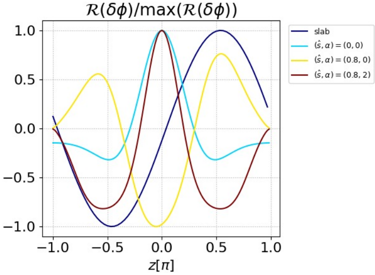

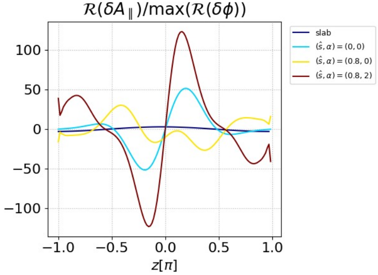

- Increase **complexity** further to better approximate a realistic tokamak: **magnetic shear + Shafranov shift.**

$$\hat{s} = \frac{r}{q}\frac{\mathrm{d}q}{\mathrm{d}r}, \qquad \alpha = -R_0 q^2 \frac{8\pi}{B_0^2}\frac{\mathrm{d}p}{\mathrm{d}r}$$

Inching towards the torus

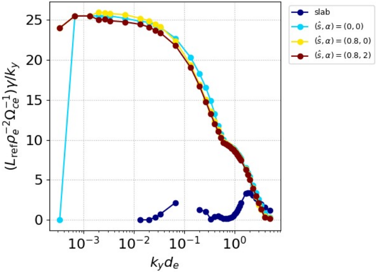

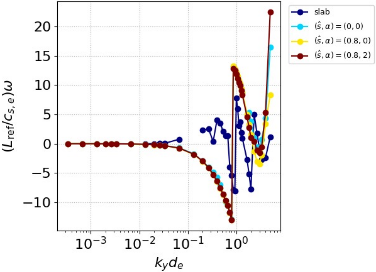

- Increase **complexity** further to better approximate a realistic tokamak: **magnetic shear + Shafranov shift.**

$$\hat{s} = \frac{r}{q}\frac{\mathrm{d}q}{\mathrm{d}r}, \qquad \alpha = -R_0 q^2 \frac{8\pi}{B_0^2}\frac{\mathrm{d}p}{\mathrm{d}r}$$

- It appears that the TAI instability mechanism appears to survive (some of) the transition to toroidicity.

Comparison with KBM and MTM

- Use "fingerprinting" to identify and class instabilities (see, e.g., Kotschenreuther et al., 2019)

	MTM	KBM	sTAI	cTAI
Parity	Odd	Even		
Drift direction	Electron	Ion		
θ behaviour	Extended	Localised		
χ_i/χ_e	$\ll 1$	~ 1		
D_e/χ_e	$\ll 1$	$\lesssim 1$		

Comparison with KBM and MTM

- Use "fingerprinting" to identify and class instabilities (see, e.g., Kotschenreuther et al., 2019)

	MTM	KBM	sTAI	cTAI
Parity	Odd	Even	Odd	Even
Drift direction	Electron	Ion		
θ behaviour	Extended	Localised		
χ_i/χ_e	$\ll 1$	~ 1		
D_e/χ_e	$\ll 1$	$\lesssim 1$		

Comparison with KBM and MTM

- Use "fingerprinting" to identify and class instabilities (see, e.g., Kotschenreuther et al., 2019)

	MTM	KBM	sTAI	cTAI
Parity	Odd	Even	Odd	Even
Drift direction	Electron	Ion	Ion	Electron
θ behaviour	Extended	Localised		
χ_i/χ_e	$\ll 1$	~ 1		
D_e/χ_e	$\ll 1$	$\lesssim 1$		

Comparison with KBM and MTM

- Use "fingerprinting" to identify and class instabilities (see, e.g., Kotschenreuther et al., 2019)

	MTM	KBM	sTAI	cTAI
Parity	Odd	Even	Odd	Even
Drift direction	Electron	Ion	Ion	Electron
θ behaviour	Extended	Localised	**?**	**?**
χ_i/χ_e	$\ll 1$	~ 1		
D_e/χ_e	$\ll 1$	$\lesssim 1$		

Comparison with KBM and MTM

- Use "fingerprinting" to identify and class instabilities (see, e.g., Kotschenreuther et al., 2019)

	MTM	KBM	sTAI	cTAI
Parity	Odd	Even	Odd	Even
Drift direction	Electron	Ion	Ion	Electron
θ behaviour	Extended	Localised	**?**	**?**
χ_i/χ_e	$\ll 1$	~ 1	**?**	**?**
D_e/χ_e	$\ll 1$	$\lesssim 1$		

Comparison with KBM and MTM

- Use “fingerprinting” to identify and class instabilities (see, e.g., Kotschenreuther et al., 2019)

	MTM	KBM	sTAI	cTAI
Parity	Odd	Even	Odd	Even
Drift direction	Electron	Ion	Ion	Electron
θ behaviour	Extended	Localised	**?**	**?**
χ_i/χ_e	$\ll 1$	~ 1	**?**	**?**
D_e/χ_e	$\ll 1$	$\lesssim 1$	**?**	**?**

A minimal model of electromagnetic saturation?

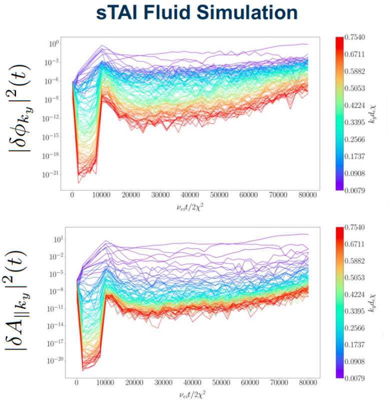

A minimal model of electromagnetic saturation?

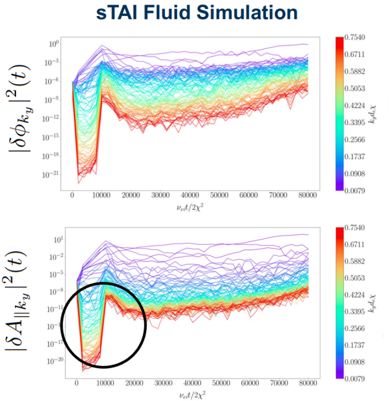

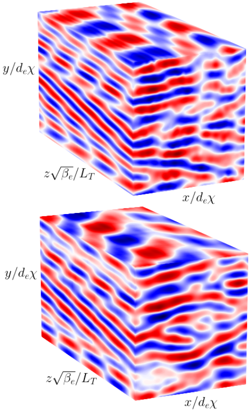

A minimal model of electromagnetic saturation?

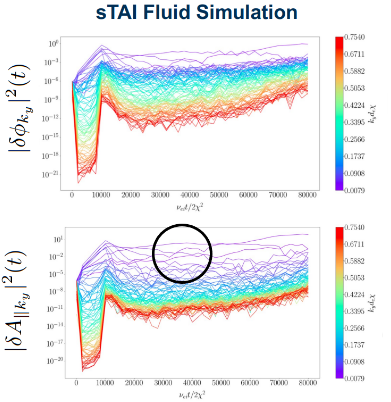

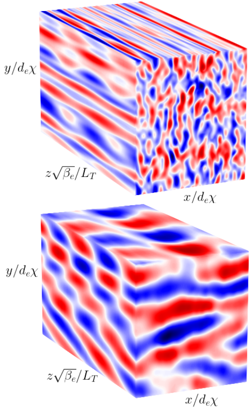

A minimal model of electromagnetic saturation?

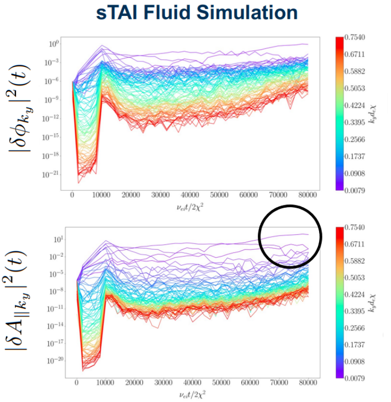

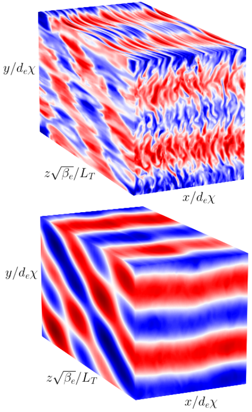

A minimal model of electromagnetic saturation?

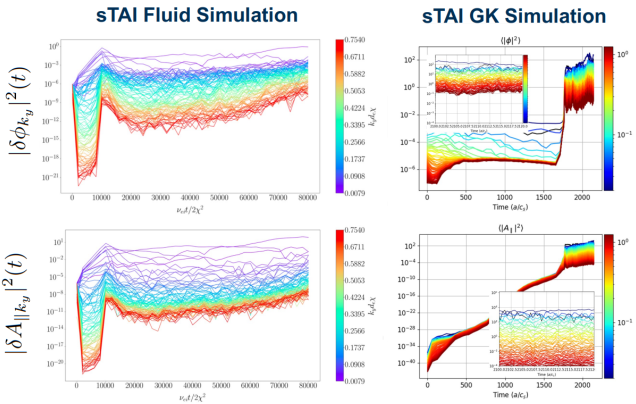

A minimal model of electromagnetic saturation?

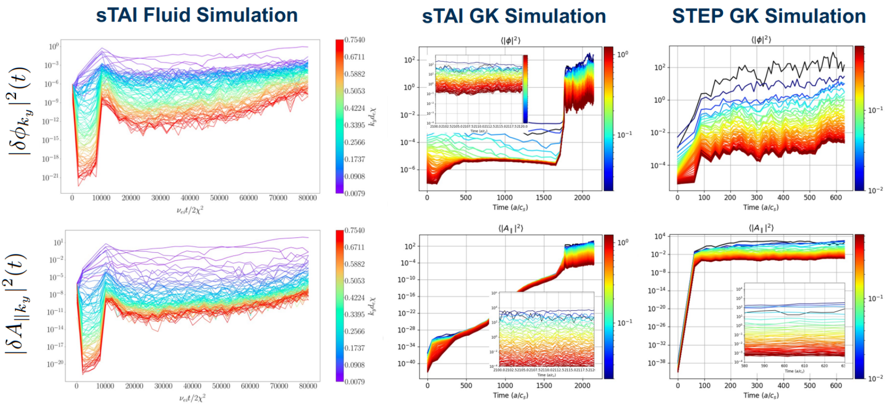

Table of Contents

Summary

- A comprehensive understanding of **electromagnetic effects** on the microinstability properties of tokamak plasmas is becoming increasingly important as experimental values of β_s will be higher in reactor-relevant tokamak scenarios.
- Complexity associated with full toroidal geometry makes progress difficult $\Rightarrow$ consider simplified models.
- The **novel thermo-Alfvénic instability (TAI)** extracts free energy from the equilibrium temperature gradient through finite perturbations to the magnetic-field direction. Two branches, slab and curvature-driven, appear to be distinct from the MTM and KBM.
- Future work: probing the robustness of its mapping from the toy model onto the torus by introducing more physics, e.g., ions, finite shaping, low-aspect ratio, etc.

Summary

- A comprehensive understanding of **electromagnetic effects** on the microinstability properties of tokamak plasmas is becoming increasingly important as experimental values of β_s will be higher in reactor-relevant tokamak scenarios.
- Complexity associated with full toroidal geometry makes progress difficult $\Rightarrow$ consider simplified models.
- The **novel thermo-Alfvénic instability (TAI)** extracts free energy from the equilibrium temperature gradient through finite perturbations to the magnetic-field direction. Two branches, slab and curvature-driven, appear to be distinct from the MTM and KBM.
- Future work: probing the robustness of its mapping from the toy model onto the torus by introducing more physics, e.g., ions, finite shaping, low-aspect ratio, etc.

Thank you for listening.
Questions?

Adkins, T., Schekochihin, A. A., Ivanov, P. G. & Roach, C. M. 2022 Electromagnetic instabilities and plasma turbulence driven by electron-temperature gradient. *J. Plasma Phys.* **88**, 905880410.

Costley, A. E. 2019 Towards a compact spherical tokamak fusion pilot plant. *Philos. Trans. R. Soc. London A* **377**, 20170439.

Giacomin, M., Kennedy, D., Casson, F. J., Ajay C., J., Dickinson, D., Patel, B. S. & Roach, C. M. 2023 On electromagnetic turbulence and transport in STEP. *Nucl. Fusion* **66**, 055010.

Horton, W., Hong, B. G. & Tang, W. M. 1988 Toroidal electron temperature gradient driven drift modes. *Phys. Fluids* **31**, 2971.

Kaye, S. M., Gerhardt, S., Guttenfelder, W., Maingi, R., Bell, R. E., Diallo, A., LeBlanc, B. P. & Podesta, M. 2013 The dependence of H-mode energy confinement and transport on collisionality in NSTX. *Nucl. Fusion* **53**, 063005.

Kennedy, D., Giacomin, M., Casson, F. J., Dickinson, D., Hornsby, W. A., Patel, B. S. & Roach, C. M. 2023 Electromagnetic gyrokinetic instabilities in STEP. *Nucl. Fusion* **63**, 126061.

Kennedy, D., Roach, C. M., Giacomin, M., Ivanov, P., Adkins, T., Sheffield, F., örler, T. G, Bokshi, A., Dickinson, D., Dudding, H. G. & Patel, B. S. 2024 On the importance of parallel magnetic-field fluctuations for electromagnetic instabilities in STEP. *arXiv e-prints* **2402.10583**.

Kotschenreuther, M., Liu, X., Hatch, D. R., Mahajan, S., Zheng, L., Diallo, A., Groebner, R., the DIII-D TEAM, Hillesheim, J. C., Maggi, C. F., Giroud, C., Koechl, F., Parail, V., Saarelma, S., Solano, E., Chankin, A. & Contributors, JET 2019 Gyrokinetic analysis and simulation of pedestals to identify the culprits for energy losses using 'fingerprints'. *Nucl. Fusion* **59**, 096001.

Pueschel, M. J., Terry, P. W., Jenko, F., Hatch, D. R., Nevins, W. M., Görler, T. & Told, D. 2013 Extreme Heat Fluxes in Gyrokinetic Simulations: A New Critical β. *Phys. Rev. Lett.* **110**, 155005.

Valovič, M., Akers, R., de Bock, M., McCone, J., Garzotti, L., Michael, C., Naylor, G., Patel, A., Roach, C. M., Scannell, R., Turnyanskiy, M., Wisse, M., Guttenfelder, W., Candy, J. & MAST Team 2011 Collisionality and safety factor scalings of H-mode energy transport in the MAST spherical tokamak. *Nucl. Fusion* **51**, 073045.